Cao *et al. Annals of Microbiology* (2025) 75:8
https://doi.org/10.1186/s13213-025-01797-8

Annals of Microbiology

UNIVERSITÀ DEGLI STUDI DI MILANO

ORIGINAL ARTICLE Open Access

Whole-genome sequencing uncovers the plant growth-promoting potential of *Bacillus licheniformis* G41, isolated from the rhizosphere soil of Gannan navel orange

Haojie Cao[1], Tao Peng[2], Wenyuan Zhao[1], Huimin Huang[1], Shuijing Yu[1*] and Yichun Zhu[1*]

Abstract

Background Gannan navel orange orchards currently rely heavily on inorganic fertilizers, which have significantly degraded soil quality. Therefore, developing sustainable methods aligned with modern green agriculture is crucial. Plant growth-promoting rhizobacteria (PGPR) are beneficial microorganisms that can promote plant growth and contribute to soil ecological balance. In-depth research and application of PGPR can support both agricultural productivity and environmental sustainability.

Results In this study, *Bacillus licheniformis* G41 was isolated from the rhizosphere soil of navel orange in southern Jiangxi Province. It was found that this strain possesses the ability to produce indole-3-acetic acid (IAA), synthesize siderophores, and solubilize phosphate. To further validate its PGP effects, strain G41 was inoculated into navel orange seedlings. After the inoculation experiment, plant height, biomass accumulation, chlorophyll content, and antioxidant enzyme activities increased in the inoculated group compared to the control group. Whole-genome sequencing revealed a genome size of 4,610,067 bp, with a total of 21 scaffolds, an average GC content of 46.17%, 4,700 predicted genes, 82 tRNAs, and 3 rRNAs. By comparing the predicted genes with the KEGG database, key functional genes related to IAA biosynthesis, siderophore biosynthesis and transport, and phosphorus cycle were identified.

Conclusion Overall, genomic analyses and PGP experiments suggest that *B. licheniformis* G41, which possesses multiple plant growth-promoting traits, can effectively promote the growth of navel orange seedlings and exhibits potential as an efficient and environmentally friendly microbial fertilizer.

Keywords *PGPR*, *Bacillus licheniformis*, *Navel orange*, *Whole-genome sequencing*

*Correspondence:
Shuijing Yu
yushuijing2008@163.com
Yichun Zhu
zhuych@jxust.edu.cn
[1]Jiangxi Provincial Key Laboratory of Environmental Pollution Prevention and Control in Mining and Metallurgy, School of Resource and Environmental Engineering, Jiangxi University of Science and Technology, Ganzhou 341000, China
[2]Yichun Strong Microbial Technology Co., Ltd, Yichun, Jiangxi 336000, China

Introduction

Navel orange is a citrus fruit belonging to the *Rutaceae* family (Xiang et al. 2020). The Gannan navel variety is widely grown in Ganzhou City, Jiangxi Province, China, and has been awarded as a national geographic indication fruit because of its appealing appearance, delicious taste, and high nutritional value (Zhang et al. 2022). However, in recent years, the soil quality of navel orange orchards has suffered an unprecedented deterioration due to irrational fertilization strategies and negligence of agricultural management, which have drastically reduced the soil health and the yield of navel orange (Zhou et al. 2021). Therefore, there is an urgent need to explore and develop an environmentally friendly and efficient method to improve the soil quality of navel orange orchards and to promote the growth of this crop.

Plant growth-promoting rhizobacteria (PGPR) are beneficial to agriculture due to their cost-effectiveness, practicality, and sustainability(Bhat et al. 2023; Perveen et al. 2023; Nagrale et al. 2023), making them increasingly attractive for both researchers and farmers. PGPR live freely in the soil or associate with plant roots, promoting plant growth by secreting specific compounds while inhibiting the growth of other harmful bacteria. The growth-promotion effect of these microorganisms on plants can be classified into two categories. The first is direct growth-promotion, in which microorganisms can increase nutrient availability (phosphate solubilization, potassium solubilization, and nitrogen fixation), secrete growth-regulating molecules (indole-3-acetic acid, 1-aminocyclopropane-1-carboxylate deaminase, gibberellins, abscisic acid), and produce siderophores. The second is indirect promotion, in which PGPR recruit other beneficial microorganisms, inhibit pathogen proliferation, improve soil conditions, and mitigate abiotic stresses (Zhou et al. 2023). A variety of PGPR have been identified, including *Azospirillum*, *Azotobacter*, *Gluconacetobacter*, *Pseudomonas*, *Bacillus*, *Burkholderia*, *Serratia*, *Streptomyces*, *Coniothyrium*, *Erwinia*, *Flavobacterium*, *Agrobacterium*, and *Trichoderma*, etc. (Gray and Smith 2005; Tabassum et al. 2017; Fadiji et al. 2022). The abundance of these microbial resources offers a wide range of applications and innovation possibilities for agricultural production.

Bacillus spp. is regarded as one of the most promising PGPR due to its ability to promote plant growth (Woo et al. 2007; Berg et al. 2014; Qessaoui et al. 2019). These bacteria are now widely applied in the fields of food (Kim et al. 2024), medicine (Irshad et al. 2018), and agriculture (Khan et al. 2022). In this study, *Bacillus licheniformis* G41 was isolated from the rhizosphere soil of Gannan navel orange. The strain was found to possess the ability to produce IAA, secrete siderophores, and to solubilize phosphate. In order to validate the effectiveness of the strain in practical application, it was inoculated into the roots of navel orange seedlings, and its impact on plant growth was monitored. This approach not only verifies the growth-promoting properties observed under laboratory conditions but also aims to provide evidence for future field applications. Although PGPR have shown potential in the agricultural field, the molecular mechanisms underlying their growth-promoting traits remain to be fully elucidated. To address this, whole-genome sequencing technology was used to conduct an in-depth analysis of functional genes involved in the regulation of plant growth, thus laying a solid genetic foundation for future agricultural biotechnology development.

Materials and methods

Collection of soil samples

The soil samples were collected from a navel orange orchard in Ganzhou City, Jiangxi Province, China (25°48′N, 115°09′E). The orchard was divided into six different areas, with five high-yield navel orange trees selected as sampling objects in each area. Rhizosphere soil was collected near the drip line of the selected navel orange trees, placed in sterile sealable bags and immediately brought back to the laboratory, where they were stored in a refrigerator at 4 °C for future use.

Isolation and purification of isolates

Soil samples collected from the same area were mixed. After mixing uniformly, 5 g of the soil sample were poured into a conical flask containing 95 mL of sterile water. The conical flask with the soil suspension was placed in a constant temperature oscillating water bath and heat for 15 min (80 °C, 180 r/min). After the treatment, the flask was left to rest for 20 min. The soil suspension was then diluted using a serial dilution method. Then, 100 μL from each dilution was plated on LB solid medium plates, in triplicate. The inoculated plates were incubated at 37 °C. Finally, single colonies with distinct morphologies were selected and purified three times on LB solid medium. The purified strains were then inoculated onto LB slant medium and stored at a low temperature for subsequent experiments.

Characterization of PGP properties

The ability of the strain to secrete IAA was determined by the Salkowski assay (Glickmann and Dessaux 1995). The isolated strain was inoculated into LB liquid medium with 100 mg/L L-tryptophan and incubated for 24 h at 37 °C, shaking at 150 r/min. The bacterial suspension (10 mL) was then centrifuged at 8000 r/min for 10 min. The supernatant was combined with Salkowski reagent at the ratio of 1:1 by volume, incubated in the dark for 30 min, and the absorbance of the mixture was measured

at 530 nm. Finally, the IAA content was calculated based on a standard curve.

Siderophore production was quantified as in Payne's method (Payne 1994), in MSA medium (Meng et al. 2022). The strain was cultured in MSA medium at 37 °C under agitation at 180 r/min for 48 h. After that, 10 mL of the culture was centrifuged at 8000 r/min for 10 min, and 2 mL of the supernatant were mixed with 2 mL of the CAS assay solution. After 1 h, OD630 nm (denoted as As) was determined. As a negative control/baseline (denoted as Ar), 2 mL of CAS assay solution was mixed with 2 mL of supernatant from uninoculated MSA medium and measured as described above. The siderophores yield was quantified in siderophore units (SU) according to the formula: SU (%) = [(Ar - As) / Ar] × 100%.

To determine phosphate solubilization ability, inorganic phosphorus medium was prepared as in (Liu et al. 2014). The strain was inoculated in 50 ml liquid medium in a conical flask and incubated at 37 °C with shaking at 180 r/min for 7 days. At the end of the experiment, the liquid medium was centrifuged at 8000 r/min for 10 min, and finally the available phosphorus content of the supernatant was determined according to the Mo-Sb anti-spetrophotometry method (Huang et al. 2010).

In-soil PGP experiment design

Navel orange seedlings of uniform size, robust growth, and free from disease or injury were purchased from a local nursery in Ganzhou City. They were cultivated in red soil, one of the four major soil types in southern Jiangxi Province. One of the isolated strains was cultured in 50 ml of liquid LB medium at 37 °C under agitation at 180 r/min until reaching the logarithmic stage. Then the preinoculum was inoculated into fresh liquid LB medium and incubated under the same conditions (37 °C, 180 r/min) for 24 h. The bacterial culture was diluted to the required OD600 of 1 by adding an appropriate amount of sterile water. The strain-inoculated experimental group and the uninoculated control group, each counted six replicates, totaling 12 pots. The experiment was carried out on the rooftop canopy of Yifu Building, Gold Campus, Jiangxi University of Science and Technology, over a period of nine weeks. Seedlings in the experimental group were inoculated weekly with 200 mL of the bacterial solution, while the control group received sterile liquid LB medium in the same manner. Daily watering was conducted, with the frequency adjusted based on actual weather conditions.

Evaluation of in-soil PGP effect

Plant height, above-ground biomass, and below-ground biomass of navel orange seedlings were measured as in (Zong and Wang 2011): (1) Plant height was measured from the graft union to the highest point of the navel orange seedlings; (2) The fresh weight of above-ground and below-ground biomass was recorded after washing the soil from the roots with water. The content of chlorophyll in the leaves was determined using the ethanol extraction method as described by Lichtenthaler and Wellburn (Lichtenthaler and Wellburn 1983). Superoxide dismutase (SOD) was determined by the SOD kit of Nanjing Jiancheng Bioengineering Institute. Peroxidase (POD) and catalase (CAT) activity were measured using POD activity detection kit and CAT activity detection kit of Beijing Solarbio Science & Technology Co., Ltd.

Whole-genome sequencing and analysis

In this study, de novo sequencing technology was employed for the whole-genome sequencing of the isolated strain. This sequencing approach allows for the analysis of the bacterial genome without relying on any reference sequences, using bioinformatics tools to reconstruct the genomic sequence from scratch. The sequencing was performed using the second-generation sequencing platform, Illumina, where DNA samples were used to construct fragments with insert sizes of approximately 400 bp, followed by paired-end (PE150) and single-end sequencing with a read length of 150 bp. Each sample was sequenced to achieve a genome coverage depth of 100x, which was subsequently used to assemble multiple genomic scaffolds. Predicted genes and biological functions were annotated by comparison with reference databases. The KEGG database was used to identify the KEGG names, KO IDs, KO descriptions, and other functional annotations, providing insights into gene functions at a systemic level. The whole-genome sequencing was performed by Shanghai Majorbio Bio-Pharm Technology Co., Ltd.

According to sequencing data, 31 housekeeping genes (including *dnaG*, *frr*, *infC*, *nusA*, *pgk*, *pyrG*, *rplA*, *rplB*, *rplC*, *rplD*, *rplE*, *rplF*, *rplK*, *rplL*, *rplM*, *rplN*, *rplP*, *rplS*, *rplT*, *rpmA*, *rpoB*, *rpsB*, *rpsC*, *rpsE*, *rpsI*, *rpsJ*, *rpsK*, *rpsM*, *rpsS*, *smpB* and *tsf*) were selected for sequence alignment in the NCBI database (URL: http://blast.ncbi.nlm.nih.gov/) using the BLAST + software (version 2.3.0) (URL: http://ftp.ncbi.nlm.nih.gov/blast/executables/blast+/2.3.0/). Through this analysis, 19 strains were identified as the closest to the experimental strains at the genus level. Finally, the phylogenetic tree of the isolate was constructed using the NJ (Neighbor-Joining) method in the software MEGA (Version 10.1.7) (URL: https://www.megasoftware.net/).

Statistical analysis

All experimental data were recorded using Microsoft Excel 2013. Statistical t-test analysis of the pot experiment data was conducted using GraphPad Prism 10, and

Table 1 Plant growth-promoting properties of strain G41

PGP trait	IAA production (mg/L)	Siderophores (%)	Phosphate solubilization (mg/L)
Activity	23.22 ± 0.03	62.17 ± 0.37	100.18 ± 5.87

Fig. 1 Plant phenotype nine weeks after inoculation (CK = control group; G41 = experimental group)

the results were graphically represented. All results are presented as mean ± standard deviation (SD).

Results

Plant growth promoting activities

The screened strain exhibited a variety of growth-promoting properties (Table 1). After one day of incubation in LB liquid medium containing L-tryptophan (100 mg/L), the IAA yield of strain G41 was 23.22 ± 0.03 mg/L. The quantitative determination of siderophores was measured in siderophore units, resulting in 62.17 ± 0.37% after two days on incubation in MSA medium. The phosphate solubilization capacity of the strain was determined by the Mo-Sb anti-spetrophotometry method as 100.18 ± 5.87 mg/L.

Effect of strain inoculation on the growth of navel orange seedlings

Inoculated navel orange seedlings exhibited a significantly enhanced growth trend compared to the control group (Figs. 1 and 2), as evidenced by metrics such as plant height (Fig. 2A), above-ground biomass (Fig. 2B), and below-ground biomass (Fig. 2C). The average height of navel orange seedlings in the uninoculated control group was 55.7 cm, the above-ground and below-ground biomass weighed 49.76 g and 20.23 g, respectively. In contrast, the navel orange seedlings inoculated with the strain grew to a height of 65.8 cm, representing an increase of 18.13%; the above-ground biomass showed a significant increase of 60.14 g, corresponding to an increase of 20.86%; the below-ground biomass also showed a significant increase of 17.8%. In summary, the inoculation with the strain G41 promoted the overall growth of navel orange seedlings, with effects on biomass accumulation. The average content of chlorophyll *a* in the control group reached 0.97 mg/g, while chlorophyll *b* was 0.34 mg/g, resulting in a total average chlorophyll content of 1.31 mg/g (Fig. 2D, E and F). In contrast, the inoculated plants showed an average content of chlorophyll *a* of 1.33 mg/g and chlorophyll *b* of 0.49 mg/g, leading to a total average chlorophyll content of 1.82 mg/g and an increase of 38.93% in total chlorophyll content. The average activity levels of superoxide dismutase (SOD), peroxidase (POD), and catalase (CAT) in the control group were 819.95 U/g, 7180.55 U/g, and 323.18 U/g, respectively. In the inoculated plants, the average activity levels of SOD, POD, and CAT were 1054.77 U/g, 13552.7 U/g, and 759.36 U/g, respectively, representing an increase of 28.64%, 88.74%, and 134.97% compared to the control group. These results indicate that there were significant differences in the activities of SOD, POD, and CAT between the inoculated treatment group and the control group.

Whole-genome overview and phylogenetic analysis

To further investigate the PGP capabilities of the strain G41 at the genetic level, whole-genome sequencing was performed. The sequencing indicated that the genome size of this strain is 4,610,067 bp, with a total number of 21 scaffolds. The average GC content is 46.17%, and the total number of genes is 4,700, including 82 tRNAs and 3 rRNAs (Table 2).

The characteristics of strain G41 genome are shown in the Fig. 3. The genome is circular, with different COG functional classifications distinguished by various colors. Specifically, the CGView genomic circle map is divided into seven concentric rings, arranged from the outermost

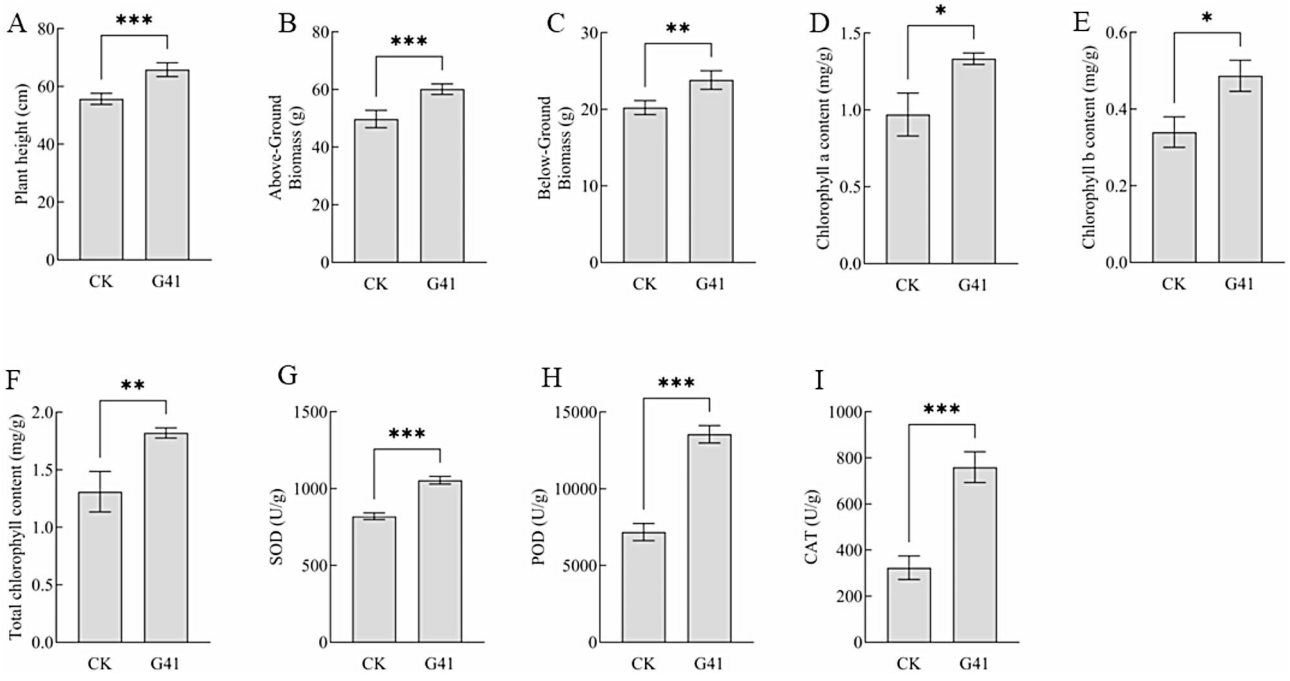

Fig. 2 Effect of inoculation with strain G41. **A**, plant height; **B**, above-ground biomass; **C**, below-ground biomass; **D**, chlorophyll *a* content; **E**, chlorophyll *b* content; **F**, total chlorophyll content; **G**, superoxide dismutase; **H**, peroxidase; **I**, catalase. The values represent the mean ± standard deviation (SD). ***, $P < 0.001$; **, $P < 0.01$; *, $P < 0.05$; ns, non-significant

Table 2 Overview of the *B. licheniformis* G41 genome

Genome size (bp)	Scaffold no.	GC content (%)	CDS no.	tRNA no.	rRNA no.
4,610,067	21	46.17	4700	82	3

to the innermost as follows: the first ring represents coding sequences (CDS) on the positive strand; the second and third rings display positive and negative strand sequence features, respectively; the fourth ring shows the CDS on the negative strand; the fifth circle displays the GC content, where outward and inward peaks indicate regions with higher and lower GC content than the genome-wide average, respectively; the sixth circle represents the GC-Skew value which is used to determine the leading and lagging strands, as well as the start and end of replication. The GC-skew is calculated using the formula: GC-skew = (G– C) / (G + C); the innermost circle represents the genome size of the strain.

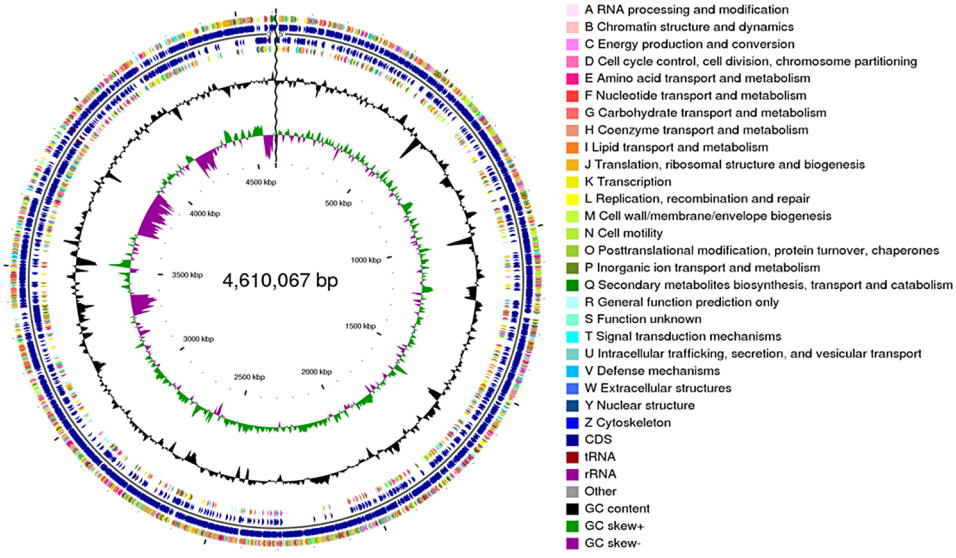

Fig. 3 CGView genomic circle map of strain G41

For the identification of the taxonomic affiliation of strain G41, its house-keeping gene sequences were analyzed against the corresponding sequences in the NCBI database using the software BlAST+. The results revealed a sequence similarity of up to 99.1% between strain G41 and Bacillus licheniformis (GCF_000011645.1). Based on these alignment results, strain G41 was classified as *Bacillus licheniformis* and accordingly named *Bacillus licheniformis* G41. A phylogenetic tree was constructed by the software MEGA as shown in Fig. 4.

Functional annotation of the strain genome

The 4,700 predicted genes were compared with the COG, GO, and KEGG databases to obtain corresponding functional annotations. According to the COG database annotations, 3,779 genes from strain G41 were classified into 23 specific categories. Among these, 402 genes related to carbohydrate transport and metabolism represented the most abundant functional category, followed by transcription, which included 394 genes, and amino acid transport and metabolism, involving 367 genes. The extracellular structures category showed the lowest number of annotated genes, with a total of five (Fig. 5). A total of 3,117 genes were annotated in the GO database and were assigned functional tags, covering three major types: biological process, cellular component, and molecular function, corresponding to 1,591, 1,545, and 2,471 gene annotations, respectively. Within their respective classifications, proteolysis, membrane, and ATP binding genes occupied dominant positions (Fig. 6). In the KEGG database, 3,447 genes were annotated, which were divided into 6 primary and 43 secondary categories. In the pathways of environmental information processing and metabolism, 404 and 2,616 genes were annotated, respectively. In the environmental information processing pathway, 212 and 189 genes associated with signal transduction and membrane transport accounted for 52.48% and 46.78% of the total number of genes, respectively. In the metabolism pathway, genes were predominantly found in global and overview maps, carbohydrate metabolism, and amino acid metabolism, with the relevant gene numbers being 1,019, 381, and 283, accounting for 38.95%, 14.56%, and 10.82% (Fig. 7).

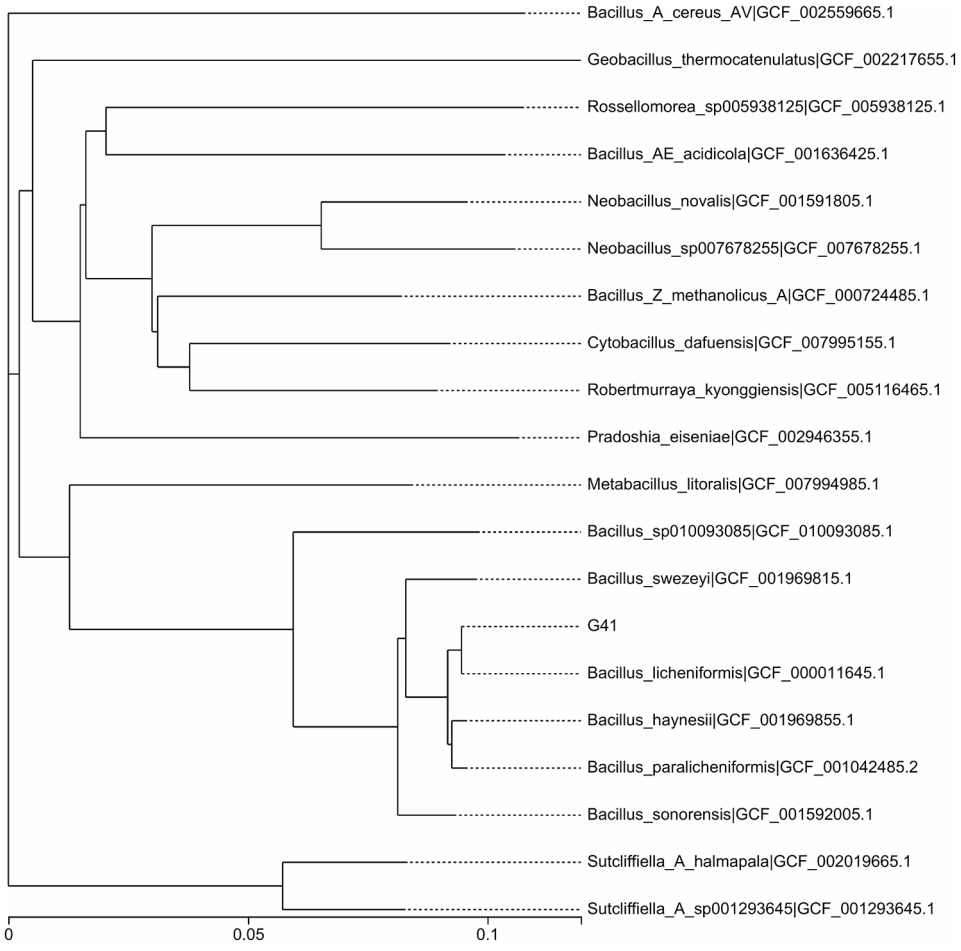

Fig. 4 Phylogenetic tree of strain G41

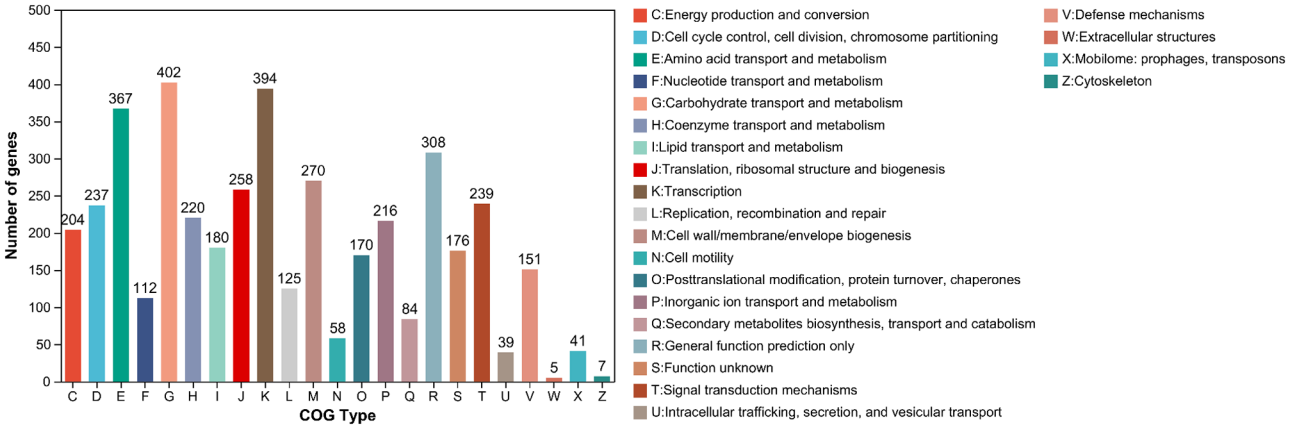

Fig. 5 COG annotation classification statistics of strain G41

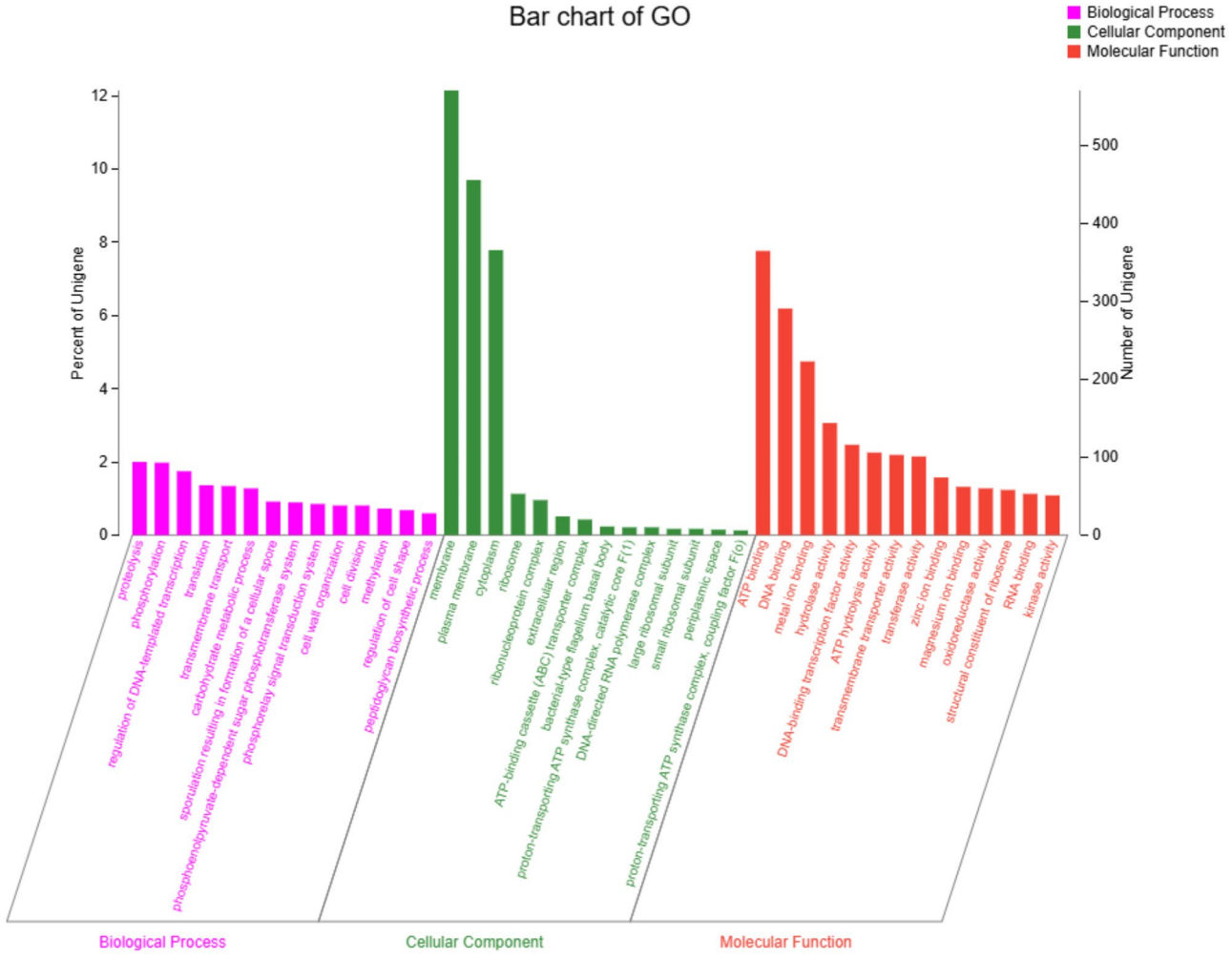

Fig. 6 GO annotation classification statistics of strain G41

Genomic mining of plant Growth-Promoting genes in B. licheniformis G41

The genome sequencing results indicate that strain G41 harbors numerous genes associated with growth-promoting properties. As shown in Table 3, a total of 39 functional genes were identified, including 9 genes involved in IAA biosynthesis, 11 genes related to siderophore biosynthesis and transport, and 19 genes

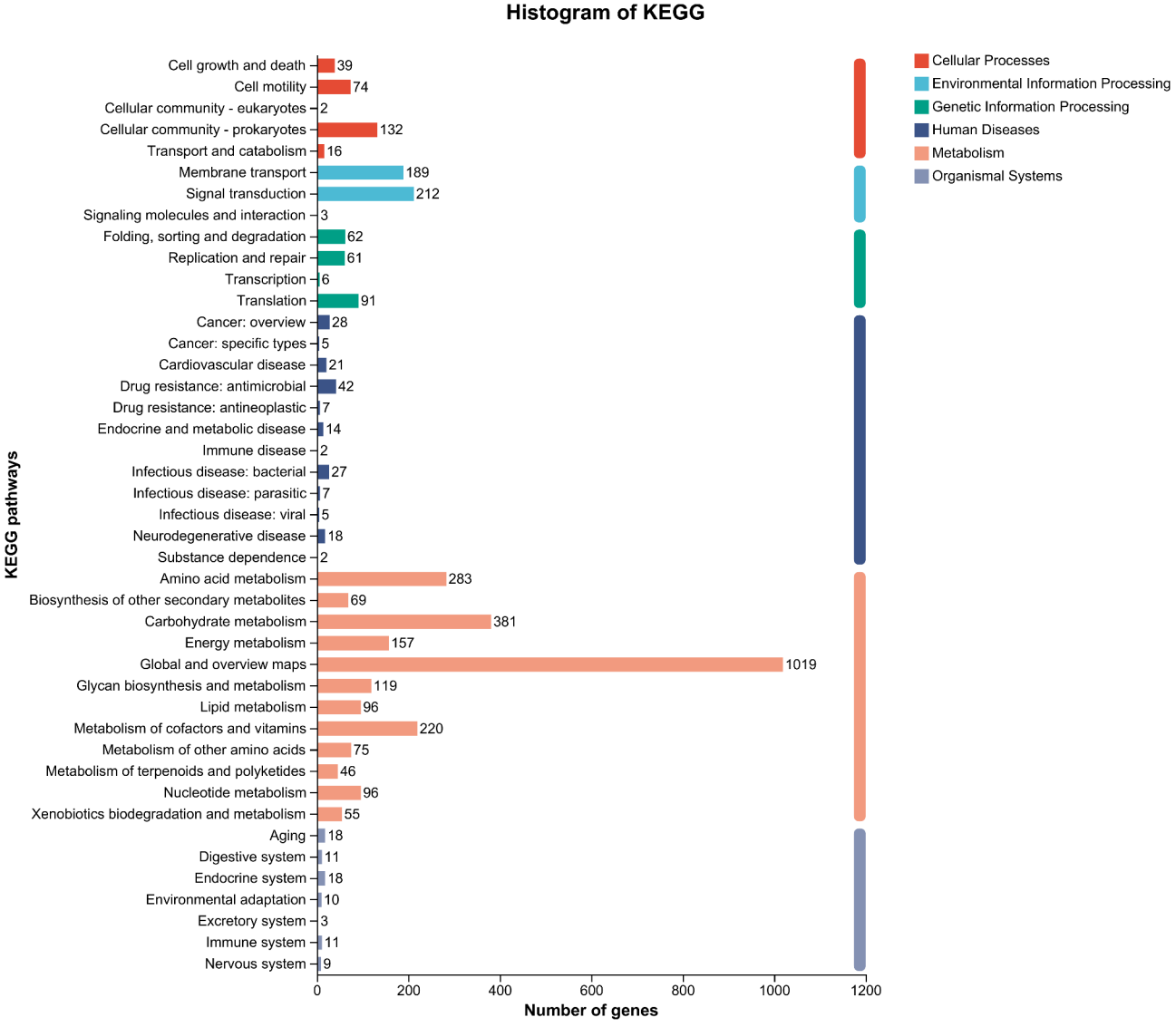

Fig. 7 KEGG pathway classification statistics of strain G41

involved in the phosphorus cycle. Among these functional genes, those related to IAA biosynthesis include *aofH*, *amiE*, a gene encoding aldehyde dehydrogenase, *trpA*, *trpB*, *trpC*, *trpD*, *trpE* and *trpF*. Monoamine oxidase plays a role in the conversion of tryptamine to indole-3-acetaldehyde in the tryptamine (TAM) pathway, amidase is able to convert indole-3-acetamide to indole-3-acetic acid in the indole-3-acetamide (IAM) pathway, and aldehyde dehydrogenase is a key enzyme in the indole-3-pyruvate (IPyA) pathway catalyzing the conversion of indole-3-acetaldehyde to indole-3-acetic acid (Tang et al. 2023). The tryptophan-linked gene *trpABCDEF* is associated with the biosynthesis of tryptophan, a precursor substance of indole-3-acetic acid (Singh et al. 2021). The genes *entABCE* (Pakarian and Pawelek 2016), *dhbF* (Abe et al. 2019), *asbA* (Lyngwi et al. 2016), and *menF* (Dahm et al. 1998)are involved in the biosynthesis of nonribosomal peptide siderophores. Three genes related to siderophores were found in the cellular ABC transporters pathway, namely *fecB*, *fecC*, and *fecD* (Braun and Herrmann 2007). The genes *hemH* is associated with the synthesis of protoporphyrin/coproporphyrin ferrochelatase in the porphyrin metabolism pathway, which is also related to siderophore production (Zhou et al. 2024). Among the phosphorus cycle genes, 6 genes related to phosphate ester mineralization were identified, specifically *glpQ* (Schwan et al. 2003), *glpA* (Schryvers and Weiner 1982), *glpK* (Rawls et al. 2011), *phoA* (Liu et al. 2018), *phoD* (Liu et al. 2018), and a 3-phytase-encoding gene (Liu et al. 2018). A total of 7 genes involved in inorganic phosphate solubilization, all related to organic acid production were also found,

Table 3 PGP trait-associated genes identified in the genome of strain G41

Function	KO ID	KO name	KO description
IAA biosynthesis	K00274	*aofH*	monoamine oxidase [EC:1.4.3.4]
	K01426	*amiE*	amidase [EC:3.5.1.4]
	K00128	-	aldehyde dehydrogenase (NAD+) [EC:1.2.1.3]
	K01695	*trpA*	tryptophan synthase alpha chain [EC:4.2.1.20]
	K01696	*trpB*	tryptophan synthase beta chain [EC:4.2.1.20]
	K01609	*trpC*	indole-3-glycerol phosphate synthase [EC:4.1.1.48]
	K00766	*trpD*	anthranilate phosphoribosyltransferase [EC:2.4.2.18]
	K01657	*trpE*	anthranilate synthase component I [EC:4.1.3.27]
	K01817	*trpF*	phosphoribosylanthranilate isomerase [EC:5.3.1.24]
Siderophore biosynthesis and transport	K00216	*entA*	2,3-dihydro-2,3-dihydroxybenzoate dehydrogenase [EC:1.3.1.28]
	K01252	*entB*	bifunctional isochorismate lyase/aryl carrier protein [EC:3.3.2.1 6.3.2.14]
	K02361	*entC*	isochorismate synthase [EC:5.4.4.2]
	K02363	*entE*	2,3-dihydroxybenzoate—[aryl-carrier protein] ligase [EC:6.3.2.14 6.2.1.71]
	K04780	*dhbF*	glyine—[glycyl-carrier protein] ligase [EC:6.2.1.66]
	K24108	*asbA*	spermidine-citrate ligase [EC:6.3.2.-]
	K02552	*menF*	menaquinone-specific isochorismate synthase [EC:5.4.4.2]
	K23181	*fecB*	ferric citrate transport system substrate-binding protein
	K23183	*fecC*	ferric citrate transport system permease protein
	K23182	*fecD*	ferric citrate transport system permease protein
	K01772	*hemH*	protoporphyrin/coproporphyrin ferrochelatase [EC:4.98.1.1 4.99.1.9]
Phosphorus cycle	K01126	*glpQ*	glycerophosphoryl diester phosphodiesterase [EC:3.1.4.46]
	K00111	*glpA*	glycerol-3-phosphate dehydrogenase [EC:1.1.5.3]
	K00864	*glpK*	glycerol kinase [EC:2.7.1.30]
	K01077	*phoA*	alkaline phosphatase [EC:3.1.3.1]
	K01113	*phoD*	alkaline phosphatase D [EC:3.1.3.1]
	K01083	-	3-phytase [EC:3.1.3.8]
	K00034	*gdh*	glucose 1-dehydrogenase [EC:1.1.1.47]
	K00925	*ackA*	acetate kinase [EC:2.7.2.1]
	K01647	*gltA*	citrate synthase [EC:2.3.3.1]
	K00873	*pyk*	pyruvate kinase [EC:2.7.1.40]
	K01958	*pyc*	pyruvate carboxylase [EC:6.4.1.1]
	K00929	*buk*	butyrate kinase [EC:2.7.2.7]
	K00891	*aroK*	shikimate kinase [EC:2.7.1.71]
	K02038	*pstA*	phosphate transport system permease protein
	K02036	*pstB*	phosphate transport system ATP-binding protein [EC:7.3.2.1]
	K02037	*pstC*	phosphate transport system permease protein
	K02040	*pstS*	phosphate transport system substrate-binding protein
	K07636	*phoR*	two-component system, OmpR family, phosphate regulon sensor histidine kinase PhoR [EC:2.7.13.3]
	K07658	*phoP*	two-component system, OmpR family, alkaline phosphatase synthesis response regulator PhoP

including *gdh*, *ackA*, *gltA*, *pyk*, *pyc*, *buk*, and *aroK* (Guo 2024). Additionally, genes encoding proteins of the high-affinity inorganic phosphate transport system, namely *pstA*, *pstB*, *pstC*, and *pstS* (Liu et al. 2018) were found, along with phosphate starvation-induced response regulatory genes *phoR* (Liu et al. 2018) and *phoP* (Choi et al. 2009).

Discussion

In this work, a strain capable of producing IAA, siderophores, and solubilizing phosphate was isolated from a navel orange orchard in the Gannan region. The strain was inoculated into the roots of navel orange seedlings in a in-soil experiment, and the results suggested its effectiveness in promoting various plant traits. This finding is consistent with numerous literature reports, about the important role of Bacillus spp. in promoting plant growth. Specifically, Shin et al. found that *B. velezensis*

BS1, capable of producing hydrolytic enzymes (cellulase and protease) and siderophores, could promote the growth of pepper seedlings (Shin et al. 2021). Similarly, Sharma et al. isolated the strain *B. subtilis* KU21 from the roots of *Rosmarinus officinalis*, which exhibited phosphate solubilization, nitrogen fixation, IAA and siderophores production, hydrogen cyanide (HCN) production, lytic enzyme activity, and ACC deaminase activity; furthermore, growth-promoting experiments on tomato showed enhanced seed germination, nutrient acquisition, and soil quality parameters (NPK) compared to the control group (Sharma et al. 2024). Devi et al. recovered two plant growth-promoting *Bacillus* strains (*B. licheniformis* MNNITSR2 and *B. velezensis* MNNITSR18) with multiple growth-promoting traits, which were found to significantly increase rice plant height, root length, root number, tiller number, leaf number, dry weight, and yield in both single inoculation and mixed inoculation treatment groups as compared to the control in a subsequent pot experiment.(Devi et al. 2023). A recent study proved that inoculating *B. subtilis* CG-6 not only significantly increased the plant height, root length, fresh weight, and dry weight of alfalfa but also significantly increased the levels of antioxidant enzymes in alfalfa leaves, with increases ranging from 15.52 to 34.03% (Chen et al. 2024).

As the earliest discovered plant hormones, indole-3-acetic acid (IAA, also known as indoleacetic acid or auxin) is an indispensable key factor in the regulation of plant growth and development (Brown 1974; Teale et al. 2006; Spaepen and Vanderleyden 2011). It is worth noting that the existence of this biologically active substance is not limited to plants, and a variety of microorganisms, including bacteria (Kang et al. 2023), yeasts (Soponputtaporn et al. 2024), and fungi (Abdelhamid et al. 2024), have also been found to possess the ability to synthesize IAA. Delving deeper into the mechanism of microbial synthesis of IAA, five major L-tryptophan-dependent pathways have been revealed in the existing literature: indole-3-acetamide (IAM), indole-3-acetonitrile (IAN), tryptophan side-chain oxidase (TSO), tryptamine (TAM), and indole-3-pyruvic acid (IPyA) (Etesami and Glick 2024). In this study, strain G41 had key genes on the three pathways of IAM, TAM, and IPyA, as well as tryptophan-linked gene. Similar to our results, Ji et al. observed a complete IPyA pathway in the whole-genome sequencing analysis of *B. amyloliquefaciens* Ba13 (Ji et al. 2021). In addition, Batista et al. found the presence of two synthesis pathways (IPyA and TAM) in *B. thuringiensis* RZ2MS9 (Batista et al. 2021). In the research field of *Lysinibacillus*, the genes *amiE* and *aldH* related to the IAM and IPyA pathways (Hilário et al. 2024), and found the key genes of the IPyA and TAM pathways (Pantoja-Guerra et al. 2023). The genome annotation of *Bacillus subtilis* confirmed the presence of the tryptophan-linked gene *trpABCDEFS* (Fang et al. 2023).

Siderophores are low-molecular-weight compounds synthesized by bacteria, actinomycetes, fungi, certain algae, and plants under iron-limiting conditions and are unique in their ability to specifically chelate Fe^{3+}, thereby effectively alleviating the pressure of iron deficiency (Kumar et al. 2018). To date, over 500 compounds have been identified as belonging to the siderophores family, which can be primarily classified into three major types based on the chemical groups that chelate trivalent iron ions: catecholate siderophores, hydroxamate siderophores, and carboxylate siderophores (Boukhalfa and Crumbliss 2002). In the process of exploring the mechanisms of siderophores synthesis, Sheng et al. firstly analyzed the siderophores synthesis genes of *Brevibacillus brevis* GZDF3 using genome mining technology and constructed the phylogenetic tree of each synthesis gene, respectively, and ultimately confirmed the strain's ability to produce catechol-type siderophores using CAS liquid phase detection and the Arnow method (Sheng et al. 2018). Moreover, the whole-genome sequencing results of *B. subtilis* TY-1 also contained a cluster of genes related to the synthesis of bacillibactin, a catechol-type siderophore (Tian et al. 2023). Chandwani et al. sequenced the whole-genome of a strain of *B. subtilis* (CWTS 5) and identified a number of genes involved in the biosynthesis and transport of siderophores (Chandwani et al. 2023). In the present work, we systematically categorized and organized the genes related to siderophore synthesis and transport from three aspects, namely, the biosynthesis of siderophore group nonribosomal peptides, the ABC transporters pathway, and the porphyrin metabolism pathway.

Phosphate solubilizing microorganisms (PSMs) can not only effectively promote the dissolution of inorganic phosphorus (Pi) by secreting protons, organic acids, inorganic acids, and other substances but also mineralize organic phosphorus (Po) through the secretion of various phosphatases, thereby increasing the content of soluble phosphorus in the soil (Tian et al. 2021; Liu et al. 2024). This process enriches the soil's phosphorus nutrient pool and enhances the efficiency of plant uptake and utilization of available phosphorus. Xu et al. analyzed the putative mechanisms by which *B. subtilis* YB-04 promotes cucumber seedlings growth from the perspective of genome sequencing and discovered that the genome of this strain contains genes encoding proteins related to the phosphate-specific transport system (*pstA*, *pstB*, *pstC*, *pstS*), response regulatory genes under phosphate starvation conditions (*phoR*, *phoP*), and alkaline phosphatase genes (*phoA*, *phoD*), which collectively constituted the strategy for the strain to adapt to a low-phosphorus environment (Xu et al. 2022). Another article

not only identified genes encoding multiple phosphatases as well as proteins related to the phosphate-specific transport system but also found several genes involved in the secretion of organic acids (Zhao et al. 2022). The high affinity phosphate transport system pstABCS can be utilized under environmental conditions in which phosphate is limiting (Martín and Liras 2021). The phosphate starvation response regulation in strain G41 is putatively regulated by the two-component regulatory system phoR-phoP. *PhoR* responds to phosphate deficiency by phosphorylating *phoP*, and the phosphorylated *phoP* then binds to specific sequences on DNA, precisely activating or repressing the transcription of genes (Santos-Beneit 2015). The regulation and expression of this key genes provide valuable insights into the molecular mechanisms of the phosphorus cycle in the microbe-soil-plant system.

Conclusion

This study focused on the microbial resources in the rhizosphere soil of Gannan navel orange. A bacterial strain named G41 was isolated and was found to possess the capability to produce IAA, siderophores, and solubilize phosphate. Further validation through pot experiments showed that inoculation with strain G41 increased the plant height, biomass, chlorophyll content, and antioxidant enzyme activities of navel orange seedlings, suggesting it to possess PGP capabilities in vivo. Subsequently, whole-genome sequencing of strain G41 was performed. Based on the analysis of housekeeping genes, the strain was identified as *Bacillus licheniformis* and officially designated as *Bacillus licheniformis* G41. Notably, this strain harbors a rich repository of functional genes, and this work found a total of 39 genes associated with PGP, which are broadly distributed across key processes of IAA biosynthesis, siderophore biosynthesis and transport, and the phosphorus cycle. In summary, *B. licheniformis* G41 holds great potential for application as a biofertilizer in sustainable agriculture. The whole-genome sequencing provides a solid theoretical foundation for further investigation into the genetic mechanisms underlying its plant growth-promoting activities.

Acknowledgements
Not applicable.

Author contributions
H.C. designed and implemented experiments, conducted data analysis, and drafted the initial manuscript. T.P. assisted with experiments execution and participated in data analysis. W.Z. assisted in the conduct of the experiments and provided technical support. H.H. contributed to data interpretation and offered critical feedback on the manuscript. S.Y. and Y.Z. as the corresponding authors, supervised the entire project, designed the experiments, and revised the manuscript. All authors have read and agreed to the published version of the manuscript.

Funding
This study was funded by the Key Research and Development Project of Ganzhou Science and Technology Bureau (2022B-NY9223).

Data availability
The research data supporting this publication are available through the data platform of Shanghai Majorbio Bio-Pharm Technology Co., Ltd. (https://www.majorbio.com/). All other relevant data supporting the findings of this study are available from the corresponding author upon reasonable request.

Declarations

Ethics approval and consent to participate
Not applicable.

Consent for publication
Not applicable.

Competing interests
The authors declare that they have no competing interests.

Received: 21 October 2024 / Accepted: 28 March 2025
Published online: 11 April 2025

References

Abdelhamid SA, Abo Elsoud MM, El-Baz AF et al (2024) Optimisation of Indole acetic acid production by *Neopestalotiopsis Aotearoa* endophyte isolated from *Thymus vulgaris* and its impact on seed germination of *Ocimum Basilicum*. BMC Biotechnol 24:46. https://doi.org/10.1186/s12896-024-00872-3

Abe T, Kobayashi K, Kawamura S et al (2019) Dipeptide synthesis by internal adenylation domains of a multidomain enzyme involved in nonribosomal peptide synthesis. J Gen Appl Microbiol 65:1–10. https://doi.org/10.2323/jgam.2018.03.001

Batista BD, Dourado MN, Figueredo EF et al (2021) The auxin-producing *Bacillus Thuringiensis* RZ2MS9 promotes the growth and modifies the root architecture of tomato (*Solanum lycopersicum* Cv. Micro-Tom). Arch Microbiol 203:3869–3882. https://doi.org/10.1007/s00203-021-02361-z

Berg G, Grube M, Schloter M, Smalla K (2014) Unraveling the plant microbiome: looking back and future perspectives. Front Microbiol 5:148. https://doi.org/10.3389/fmicb.2014.00148

Bhat MA, Mishra AK, Jan S et al (2023) Plant growth promoting rhizobacteria in plant health: a perspective study of the underground interaction. Plants 12:629. https://doi.org/10.3390/plants12030629

Boukhalfa H, Crumbliss AL (2002) Chemical aspects of siderophore mediated iron transport. Biometals 15:325–339. https://doi.org/10.1023/A:1020218608266

Braun V, Herrmann C (2007) Docking of the periplasmic FecB binding protein to the FecCD transmembrane proteins in the ferric citrate transport system of *Escherichia coli*. J Bacteriol 189:6913–6918. https://doi.org/10.1128/jb.00884-07

Brown ME (1974) Seed and root bacterization. Annu Rev Phytopathol 12:181–197. https://doi.org/10.1146/annurev.py.12.090174.001145

Chandwani S, Dewala S, Chavan SM et al (2023) Complete genome sequencing of *Bacillus subtilis* (CWTS 5), a siderophore-producing bacterium triggers antagonistic potential against *Ralstonia solanacearum*. J Appl Microbiol 134:1–14. https://doi.org/10.1093/jambio/lxad066

Chen J, Cai R, Tang L et al (2024) Antagonistic activity and mechanism of *Bacillus subtilis* CG-6 suppression of root rot and growth promotion in alfalfa. Microb Pathog 190:106616. https://doi.org/10.1016/j.micpath.2024.106616

Choi E, Groisman EA, Shin D (2009) Activated by different signals, the PhoP/PhoQ two-component system differentially regulates metal uptake. J Bacteriol 191:7174–7181. https://doi.org/10.1128/jb.00958-09

Dahm C, Müller R, Schulte G et al (1998) The role of isochorismate hydroxymutase genes *EntC* and *MenF* in Enterobactin and menaquinone biosynthesis in *Escherichia coli*. Biochim Et Biophys Acta (BBA) - Gen Subj 1425:377–386. https://doi.org/10.1016/S0304-4165(98)00089-0

Devi S, Sharma S, Tiwari A et al (2023) Screening for multifarious plant growth promoting and biocontrol attributes in *Bacillus* strains isolated from Indo gangetic soil for enhancing growth of rice crops. Microorganisms 11:1085. https://doi.org/10.3390/microorganisms11041085

Etesami H, Glick BR (2024) Bacterial indole-3-acetic acid: a key regulator for plant growth, plant-microbe interactions, and agricultural adaptive resilience. Microbiol Res 281:127602. https://doi.org/10.1016/j.micres.2024.127602
Fadiji AE, Babalola OO, Santoyo G, Perazzolli M (2022) The potential role of microbial biostimulants in the amelioration of climate change-associated abiotic stresses on crops. Front Microbiol 12:829099. https://doi.org/10.3389/fmicb.2021.829099
Fang L, Zheng X, Sun Z et al (2023) Characterization of a Plant Growth-Promoting Endohyphal *Bacillus subtilis* in *Fusarium acuminatum* from *Spiranthes sinensis*. Polish Journal of Microbiology 72:29–37. https://doi.org/10.33073/pjm-2023-007
Glickmann E, Dessaux Y (1995) A critical examination of the specificity of the Salkowski reagent for Indolic compounds produced by phytopathogenic bacteria. Appl Environ Microbiol 61:793–796. https://doi.org/10.1128/aem.61.2.793-796.1995
Gray EJ, Smith DL (2005) Intracellular and extracellular PGPR: commonalities and distinctions in the plant–bacterium signaling processes. Soil Biol Biochem 37:395–412. https://doi.org/10.1016/j.soilbio.2004.08.030
Guo XD (2024) Isolation and identification of two strains of phosphorus-solubilizing bacteria in the rhizosphere of Gannan navel orange and their phosphorus-solubilizing mechanism. Jiangxi Univ Sci Technol. https://doi.org/10.27176/d.cnki.gnfyc.2023.000918
Hilário S, Gonçalves MFM, Matos I et al (2024) Comparative genomics reveals insights into the potential of *Lysinibacillus Irui* as a plant growth promoter. Appl Microbiol Biotechnol 108:370. https://doi.org/10.1007/s00253-024-13210-6
Huang J, Sheng XF, He LY (2010) Biodiversity of phosphate-dissolving and plant growth-promoting endophytic bacteria of two crops. Acta Microbiol Sinica 50:710–716. https://doi.org/10.13343/j.cnki.wsxb.2010.06.002
Irshad F, Mushtaq Z, Akhtar S (2018) Sequence analysis and comparative bioinformatics study of Camelysin gene (*calY*) isolated from *Bacillus Thuringiensis*. Biochem Genet 56:103–115. https://doi.org/10.1007/s10528-017-9833-6
Ji C, Zhang M, Kong Z et al (2021) Genomic analysis reveals potential mechanisms underlying promotion of tomato plant growth and antagonism of soilborne pathogens by *Bacillus amyloliquefaciens* Ba13. Microbiol Spectr 9:e01615–e01621. https://doi.org/10.1128/Spectrum.01615-21
Kang S-M, Hoque MIU, Woo J-I, Lee I-J (2023) Mitigation of salinity stress on soybean seedlings using Indole acetic acid-producing *Acinetobacter Pittii* YNA40. Agriculture 13:1021. https://doi.org/10.3390/agriculture13051021
Khan AR, Mustafa A, Hyder S et al (2022) *Bacillus* spp. As bioagents: uses and application for sustainable agriculture. Biology 11:1763. https://doi.org/10.3390/biology11121763
Kim JH, Lee ES, Kim BM et al (2024) Simple purification and antimicrobial properties of bacteriocin-like inhibitory substance from *Bacillus* species for the biopreservation of cheese. Foods 13:10. https://doi.org/10.3390/foods13010010
Kumar P, Thakur S, Dhingra GK et al (2018) Inoculation of siderophore producing rhizobacteria and their consortium for growth enhancement of wheat plant. Biocatal Agric Biotechnol 15:264–269. https://doi.org/10.1016/j.bcab.2018.06.019
Lichtenthaler HK, Wellburn AR (1983) Determinations of total carotenoids and chlorophylls *a* and *b* of leaf extracts in different solvents. Biochem Soc Trans 11:591–592. https://doi.org/10.1042/bst0110591
Liu FP, Liu HQ, Zhou HL et al (2014) Isolation and characterization of phosphate-solubilizing bacteria from betel nut (*Areca catechu*) and their effects on plant growth and phosphorus mobilization in tropical soils. Biol Fertil Soils 50:927–937. https://doi.org/10.1007/s00374-014-0913-z
Liu J, Cade-Menun BJ, Yang J et al (2018) Long-term land use affects phosphorus speciation and the composition of phosphorus cycling genes in agricultural soils. Front Microbiol 9. https://doi.org/10.3389/fmicb.2018.01643
Liu F, Qian J, Zhu Y et al (2024) Phosphate solubilizing microorganisms increase soil phosphorus availability: a review. Geomicrobiol J 41:1–16. https://doi.org/10.1080/01490451.2023.2272620
Lyngwi NA, Nongkhlaw M, Kalita D, Joshi SR (2016) Bioprospecting of plant growth promoting bacilli and related genera prevalent in soils of pristine sacred Groves: biochemical and molecular approach. PLoS ONE 11:e0152951. https://doi.org/10.1371/journal.pone.0152951
Martín JF, Liras P (2021) Molecular mechanisms of phosphate sensing, transport and signalling in *Streptomyces* and related actinobacteria. Int J Mol Sci 22:1129. https://doi.org/10.3390/ijms22031129
Meng JY, Guo HQ, Jia LJ et al (2022) Analysis of phosphate-solubilizing endophytic bacteria taxa and their phosphate-solubilizing and siderophore-producing abilities in desert shrubs of inner Mongolia. Jiangsu Agricultural Sci 50:260–264. https://doi.org/10.15889/j.issn.1002-1302.2022.12.039
Nagrale DT, Chaurasia A, Kumar S et al (2023) PGPR: the treasure of multifarious beneficial microorganisms for nutrient mobilization, pest biocontrol and plant growth promotion in field crops. World J Microbiol Biotechnol 39:100. https://doi.org/10.1007/s11274-023-03536-0
Pakarian P, Pawelek PD (2016) Intracellular co-localization of the *Escherichia coli* Enterobactin biosynthetic enzymes EntA, EntB, and ente. Biochem Biophys Res Commun 478:25–32. https://doi.org/10.1016/j.bbrc.2016.07.105
Pantoja-Guerra M, Burkett-Cadena M, Cadena J et al (2023) *Lysinibacillus spp.*: an IAA-producing endospore forming-bacteria that promotes plant growth. Antonie Van Leeuwenhoek 116:615–630. https://doi.org/10.1007/s10482-023-01828-x
Payne SM (1994) Detection, isolation, and characterization of siderophores. Methods Enzymol 235:329–344. https://doi.org/10.1016/0076-6879(94)35151-1
Perveen R, Hussain A, Ditta A et al (2023) Growth and yield of Okra exposed to a consortium of rhizobacteria with different organic carriers under controlled and natural field conditions. Horticulturae 9:8. https://doi.org/10.3390/horticulturae9010008
Qessaoui R, Bouharroud R, Furze JN et al (2019) Applications of new rhizobacteria *Pseudomonas* isolates in agroecology via fundamental processes complementing plant growth. Sci Rep 9:12832. https://doi.org/10.1038/s41598-019-49216-8
Rawls KS, Martin JH, Maupin-Furlow JA (2011) Activity and transcriptional regulation of bacterial protein-like glycerol-3-phosphate dehydrogenase of the Haloarchaea in *Haloferax volcanii*. J Bacteriol 193:4469–4476. https://doi.org/10.1128/jb.00276-11
Santos-Beneit F (2015) The Pho Regulon: a huge regulatory network in bacteria. Front Microbiol 6:402. https://doi.org/10.3389/fmicb.2015.00402
Schryvers A, Weiner JH (1982) The anaerobic *sn*-glycerol-3-phosphate dehydrogenase: cloning and expression of the *glp*A gene of *Escherichia coli* and identification of the *glp*A products. Can J Biochem 60:224–231. https://doi.org/10.1139/o82-027
Schwan TG, Battisti JM, Porcella SF et al (2003) Glycerol-3-phosphate acquisition in spirochetes: distribution and biological activity of glycerophosphodiester phosphodiesterase (GlpQ) among *Borrelia* species. J Bacteriol 185:1346–1356. https://doi.org/10.1128/jb.185.4.1346-1356.2003
Sharma M, Sood G, Chauhan A (2024) Assessment of plant growth promotion potential of endophytic bacterium *B. subtilis* KU21 isolated from *Rosmarinus officinalis*. Curr Microbiol 81:207. https://doi.org/10.1007/s00284-024-03734-5
Sheng M, Jia H, Tao X et al (2018) Mining, isolation and identification of siderophore synthesis gene from *Brevibacillus brevis* GZDF3. AJBB 14:200–209. https://doi.org/10.3844/ajbbsp.2018.200.209
Shin JH, Park BS, Kim HY et al (2021) Antagonistic and plant growth-promoting effects of *Bacillus velezensis* BS1 isolated from rhizosphere soil in a pepper field. Plant Pathol J 37:307–314. https://doi.org/10.5423/PPJ.NT.03.2021.0053
Singh P, Singh RK, Guo D-J et al (2021) Whole genome analysis of sugarcane root-associated endophyte *Pseudomonas aeruginosa* B18—a plant growth-promoting bacterium with antagonistic potential against *Sporisorium Scitamineum*. Front Microbiol 12. https://doi.org/10.3389/fmicb.2021.628376
Soponputtaporn S, Srithaworn M, Promnuan Y et al (2024) Indole-3-acetic acid producing yeasts in the phyllosphere of legumes: benefits for Chili growth. Trends Sci 21:7335. https://doi.org/10.48048/tis.2024.7335
Spaepen S, Vanderleyden J (2011) Auxin and plant-microbe interactions. Cold Spring Harb Perspect Biol 3:a001438. https://doi.org/10.1101/cshperspect.a001438
Tabassum B, Khan A, Tariq M et al (2017) Bottlenecks in commercialisation and future prospects of PGPR. Appl Soil Ecol 121:102–117. https://doi.org/10.1016/j.apsoil.2017.09.030
Tang J, Li Y, Zhang L et al (2023) Biosynthetic pathways and functions of Indole-3-Acetic acid in microorganisms. Microorganisms 11:2077. https://doi.org/10.3390/microorganisms11082077
Teale WD, Paponov IA, Palme K (2006) Auxin in action: signalling, transport and the control of plant growth and development. Nat Rev Mol Cell Biol 7:847–859. https://doi.org/10.1038/nrm2020
Tian J, Ge F, Zhang D et al (2021) Roles of phosphate solubilizing microorganisms from managing soil phosphorus deficiency to mediating biogeochemical P cycle. Biology 10:158. https://doi.org/10.3390/biology10020158
Tian Y, Ji S, Zhang E et al (2023) Complete genome analysis of *Bacillus subtilis* TY-1 reveals its biocontrol potential against tobacco bacterial wilt. Mar Genom 68:101018. https://doi.org/10.1016/j.margen.2023.101018

Woo SM, Woo JU, Kim SD (2007) Purification and characterization of the siderophore from *Bacillus licheniformis* K11, a multi-functional plant growth promoting rhizobacterium. Microbiol Biotechnol Lett 35:128–134

Xiang Z, Chen X, Qian C et al (2020) Determination of volatile flavors in fresh navel orange by multidimensional gas chromatography quadrupole time-of-flight mass spectrometry. Anal Lett 53:614–626. https://doi.org/10.1080/00032719.2019.1662429

Xu W, Yang Q, Yang F et al (2022) Evaluation and genome analysis of *Bacillus subtilis* YB-04 as a potential biocontrol agent against *Fusarium* wilt and growth promotion agent of cucumber. Front Microbiol 13:885430. https://doi.org/10.3389/fmicb.2022.885430

Zhang J, Zhang J, Shan Y et al (2022) Effect of harvest time on the chemical composition and antioxidant capacity of Gannan navel orange (*Citrus sinensis* L. Osbeck 'Newhall') juice. J Integr Agric 21:261–272. https://doi.org/10.1016/S2095-3119(20)63395-0

Zhao D, Ding Y, Cui Y et al (2022) Isolation and genome sequence of a novel phosphate-solubilizing rhizobacterium *Bacillus altitudinis* GQYP101 and its effects on rhizosphere microbial community structure and functional traits of corn seedling. Curr Microbiol 79:249. https://doi.org/10.1007/s00284-022-02944-z

Zhou Y, Tang Y, Hu C et al (2021) Soil applied Ca, Mg and B altered phyllosphere and rhizosphere bacterial Microbiome and reduced Huanglongbing incidence in Gannan navel orange. Sci Total Environ 791:148046. https://doi.org/10.1016/j.scitotenv.2021.148046

Zhou YF, Bai YS, Yue T et al (2023) Research progress on the growth-promoting characteristics of plant growth-promoting rhizobacteria. Microbiol China 50:644–666. https://doi.org/10.13344/j.microbiol.china.220446

Zhou YF, Wang JB, He C et al (2024) Screening, identification and growth promotion of a strain of *Bacillus velezensis* JB0319 producing indoleacetic acid. Chin J Soil Sci 173–183. https://doi.org/10.19336/j.cnki.trtb.2023013001

Zong XF, Wang SG (2011) Plant physiology research and technology. Southwest China Normal University, Chongqing, pp 47–58

Publisher's note